OPEN

Metabolic Activation of Flavin Monooxygenase-mediated Trimethylamine-*N*-Oxide Formation in Experimental Kidney Disease

Alexander J. Prokopienko [1], Raymond E. West III[1], Daniel P. Schrum[1], Jason R. Stubbs[2], François A. Leblond [3], Vincent Pichette[4] & Thomas D. Nolin [1]*

Cardiovascular disease (CVD) remains the leading cause of death in chronic kidney disease (CKD) patients despite treatment of traditional risk factors, suggesting that non-traditional CVD risk factors are involved. Trimethylamine-*N*-oxide (TMAO) correlates with atherosclerosis burden in CKD patients and may be a non-traditional CVD risk factor. Serum TMAO concentrations are significantly increased in CKD patients, which may be due in part to increased hepatic flavin monooxygenase (FMO)-mediated TMAO formation. The objective of this work was to elucidate the mechanism of increased FMO activity in CKD. In this study, FMO enzyme activity experiments were conducted *in vitro* with liver microsomes isolated from experimental CKD and control rats. Trimethylamine was used as a probe substrate to assess FMO activity. The FMO activator octylamine and human uremic serum were evaluated. FMO gene and protein expression were also determined. FMO-mediated TMAO formation was increased in CKD versus control. Although gene and protein expression of FMO were not changed, metabolic activation elicited by octylamine and human uremic serum increased FMO-mediated TMAO formation. The findings suggest that metabolic activation of FMO-mediated TMAO formation is a novel mechanism that contributes to increased TMAO formation in CKD and represents a therapeutic target to reduce TMAO exposure and CVD.

Cardiovascular disease (CVD) events are the leading cause of death in chronic kidney disease (CKD) patients despite aggressive treatment of traditional risk factors[1], suggesting that non-traditional CVD risk factors may play an important role[2,3]. Trimethylamine-*N*-oxide (TMAO) promotes atherosclerosis in preclinical models[4], is elevated and associated with CVD in CKD patients[5–7], and may be a novel non-traditional CVD risk factor[8]. For instance, we have shown that circulating TMAO concentrations are 30-fold higher in patients with end-stage kidney disease (ESKD) than in the general population and correlate with coronary atherosclerosis burden[9]. Elevated TMAO concentrations may also directly contribute to fibrosis and non-ischemic heart failure in CKD[10–12]. TMAO concentrations increase disproportionately from Stage 4 to 5 CKD (i.e., 20 μM to 94 μM) compared to Stage 1 to 3 CKD (i.e., 3.3 μM to 10 μM)[7,9], strongly implicating formation of TMAO as a contributor to elevated serum TMAO concentrations in advanced CKD. Recently, we demonstrated that enhanced hepatic flavin monooxygenase (FMO)-mediated TMAO formation along with decreased renal clearance contributes to increased TMAO exposure in a mouse model of experimental kidney disease[13]. However, the mechanism driving increased TMAO formation remained unclear.

[1]Center for Clinical Pharmaceutical Sciences, Department of Pharmaceutical Sciences or Department of Pharmacy and Therapeutics, School of Pharmacy, University of Pittsburgh, Pittsburgh, PA, United States. [2]The Kidney Institute, and Department of Internal Medicine, Division of Nephrology & Hypertension, University of Kansas Medical Center, Kansas City, KS, United States. [3]ProMetic Life Sciences Inc., Laval, Québec, Canada. [4]Service de Néphrologie et Centre de Recherche, Hôpital Maisonneuve-Rosemont, Département de Pharmacologie, Université de Montréal, Montréal, Québec, Canada. *email: nolin@pitt.edu

Mechanistic evaluation of increased TMAO formation could shed light on novel therapeutic strategies for the prevention of CVD in CKD. In fact, recent studies provide proof of principle that FMO activity is a potential therapeutic target[14]. In mice, antisense oligonucleotide-mediated knockdown of *FMO3* (the primary isoform responsible for TMAO formation in humans) leads to decreases in serum TMAO concentrations and atherosclerosis formation[15,16]. Therapeutically targeting FMOs may be particularly effective in the setting of increased FMO-mediated TMAO formation as seen in diabetes and CKD[13,15,17].

The objective of this study was to elucidate potential mechanisms of increased hepatic FMO-mediated TMAO formation observed in CKD. We accomplished this by conducting FMO enzyme activity experiments with CKD and control rat microsomal fractions. We also investigated potential changes in mRNA and protein expression of FMOs.

Results

Characteristics of CKD and control rats. TMAO exposure was compared between CKD and control rats. The median (interquartile range) TMAO concentration in CKD versus control serum was 58 μM (31–102) and 3.4 μM (3.15–5.24), respectively ($P = 0.0022$; Fig. 1A). Serum creatinine and blood urea nitrogen (BUN) were also higher in CKD rats versus control ($P < 0.0001$; Fig. 1B).

FMO activity in CKD and control rats. The potential mechanism of altered FMO-mediated TMAO formation in CKD was assessed by comparing enzyme kinetic parameters observed in CKD rat liver microsomes with control rat microsomes. The V_{max} (i.e., the maximal rate at which the enzyme catalyzes the reaction) for TMAO formation was increased by 25% in CKD versus control (651.4 ± 18 versus 522.7 ± 22 pmol/mg protein/minute, $P < 0.0001$; Fig. 1C). The K_m value (i.e., substrate concentration at half the maximum velocity) was not different between groups (16.3 ± 2.3 versus 11.3 ± 2.5 μM, $P = 0.15$).

Gene and protein expression. In order to evaluate whether any changes in FMO activity were due to changes in gene or protein regulation, hepatic FMO mRNA and protein expression were assessed (Fig. 2A). No change in *Fmo1* or *Fmo3* mRNA was observed in CKD versus control. The positive control *Cyp(Cytochrome P450)-3a2* was downregulated in CKD versus control ($P < 0.0001$). *Ahr* (aryl-hydrocarbon receptor) was upregulated in CKD versus control ($P < 0.05$) but *Arnt* (aryl hydrocarbon receptor nuclear translocator) and *Cyp1a2* were not.

FMO3, CYP1A2, AhR and CYP3A2 protein expression is presented in Fig. 2B. Decreases in AhR ($P < 0.01$) and CYP3A2 ($P < 0.001$) but no change in FMO3 and CYP1A2 protein expression were observed in CKD versus control.

Metabolic activation and inhibition of FMO. An atypical kinetic reaction known as metabolic activation was explored as a potential mechanism of increased FMO activity. Concentration-dependent increases of up to 4-fold in metabolic activation were observed with octylamine as a positive activation control ($P < 0.0001$; Fig. 3A). L-arginine was evaluated to identify potential representative endogenous compounds responsible for activation; up to a 1.4-fold increase in metabolic activation was observed in the presence of L-arginine ($P < 0.0001$; Fig. 3B). FMO-mediated TMAO formation was decreased by 58% ($P < 0.0001$; Fig. 3C) in the presence of the FMO inhibitor methimazole. Lastly, FMO activity was determined in the presence 5–20% ultra-filtered human serum to assess whether solutes retained in ESKD can activate FMO enzymes. TMAO formation velocity was increased up to 3-fold with uremic serum compared to 1.9-fold with healthy control serum ($P < 0.0001$; Fig. 4).

Discussion

We show for the first time that metabolic activation of hepatic FMOs leads to increased formation of the non-traditional CVD risk factor TMAO, which may contribute to dramatically elevated serum concentrations in CKD rats. These findings corroborate our clinical observations of significantly elevated systemic TMAO concentrations in patients with advanced CKD and provide a novel mechanism for our recent observations of enhanced FMO-mediated TMAO formation in experimental CKD[9,13].

Mechanistically, metabolic activation of FMO enzymes by uremic solutes may contribute to increased TMAO formation in CKD. In fact, metabolic activation likely contributes to the increased systemic exposure of TMAO observed in CKD, evidenced by disproportionate increases of serum TMAO in advanced CKD relative to earlier stages of CKD. For instance, TMAO serum concentrations are increased 16-fold in CKD rats (Fig. 1B), and 30-fold in ESKD patients compared to controls[9]. The V_{max} of TMAO formation was increased by 25% ($P < 0.0001$; Fig. 1A) in CKD versus control tissue in the isolated microsomal incubation experiments. However, no changes in FMO gene or protein expression (Fig. 2A,B) were observed, suggesting that increased FMO activity was unrelated to changes in expression. The latter finding is inconsistent with our previous observations in mice, in which gene expression changes may partially explain differences in FMO activity[13], but is not unexpected given well-known species differences in FMO3 regulation in mice compared to rats and humans[18]. For instance, FMO3 expression is also profoundly decreased by testosterone in mice but this effect is less clear in rats and humans[19,20]. Therefore, the current experimental rat model may better reflect FMO3 regulation and metabolic activity observed in humans with CKD. Furthermore, changes in FMO3 mRNA and protein expression often do not correlate with serum TMAO exposure, suggesting that alternative mechanisms such as metabolic activation may regulate FMO activity[21]. Nevertheless, current and previous findings collectively indicate that FMO-mediated TMAO formation is increased in CKD, and our present data suggest that it is mechanistically driven by metabolic activation.

Metabolic activation was elicited with octylamine, L-arginine, and uremic and healthy control serum. The up to 4-fold increase in V_{max} in the presence of octylamine clearly demonstrates that FMO-mediated TMAO formation can be activated (Fig. 3A)[14]. The increased metabolic activation with human uremic serum versus healthy control serum suggests that increased concentrations of uremic solutes retained in uremic serum elicit greater metabolic activation (Fig. 4A). Although the potential effector compounds remain unknown, the endogenous
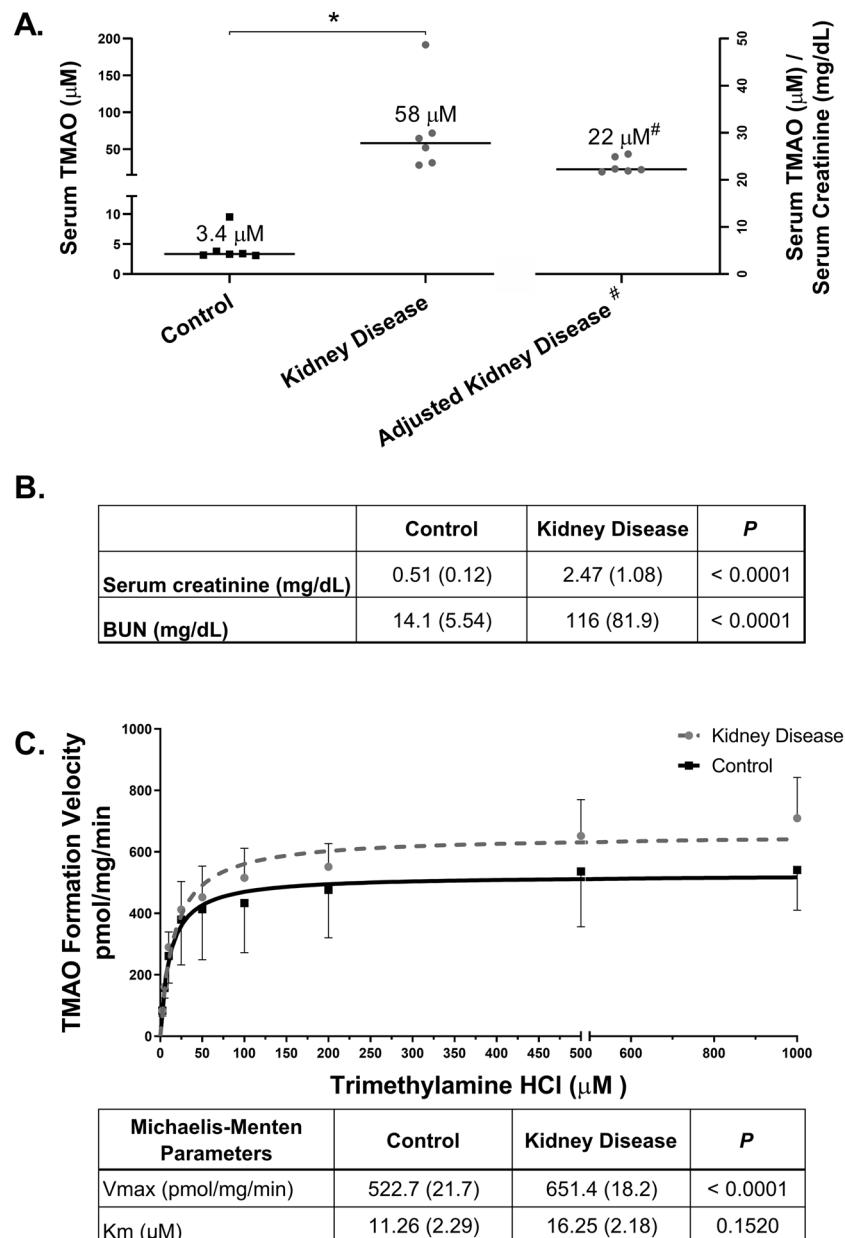
Figure 1. FMO Activity and Serum TMAO Concentrations in CKD and Control Rats. (**A**) Serum concentrations of TMAO compared between CKD (n = 6) rats and controls (n = 6). #Serum TMAO concentrations were adjusted for kidney function by dividing individual TMAO concentrations by the corresponding serum creatinine (mg/dL) values. *$P < 0.05$ for CKD compared to control with a Mann-Whitney test. (**B**) Biochemical characteristics were compared between CKD (n = 12) and controls (n = 12) with a Student's *t*-tests and presented as mean ± SD. (**C**) Michaelis-Menten plot for the formation of TMAO in rat liver microsomes of both control and CKD rats. Liver microsomal protein (0.5 mg/mL) was incubated with various concentrations of trimethylamine (2.5–1000 μM) for 60 min at 37 °C. Each point represents the mean ± SEM of 6 rats in each group. The parameters were statistically compared with an F-test.

solute L-arginine elicits activation (Fig. 3B), and other structurally similar endogenous substances may behave in a similar manner. Interestingly, L-arginine serum concentrations are similar in CKD and healthy patients[22], and it is possible that L-arginine is contributing to the metabolic activation observed with healthy control serum (Fig. 4B).

Metabolic activation is an atypical kinetic reaction. Activation of FMO-mediated TMAO formation indicates that 'effector' compounds are eliciting structural or electrostatic changes in the FMO catalytic site[23]. In fact, FMO enzymes can be activated by a broad range of effector compounds that are known uremic retention solutes, including primary amines, guanidine derivatives and small peptides[14,24,25]. In CKD, these compounds may deposit and accumulate in liver tissue, specifically in the microsomal fraction where they can act as FMO effectors[26,27], and this may explain the present findings of metabolic activation and increased TMAO formation in experimental CKD[28–32].
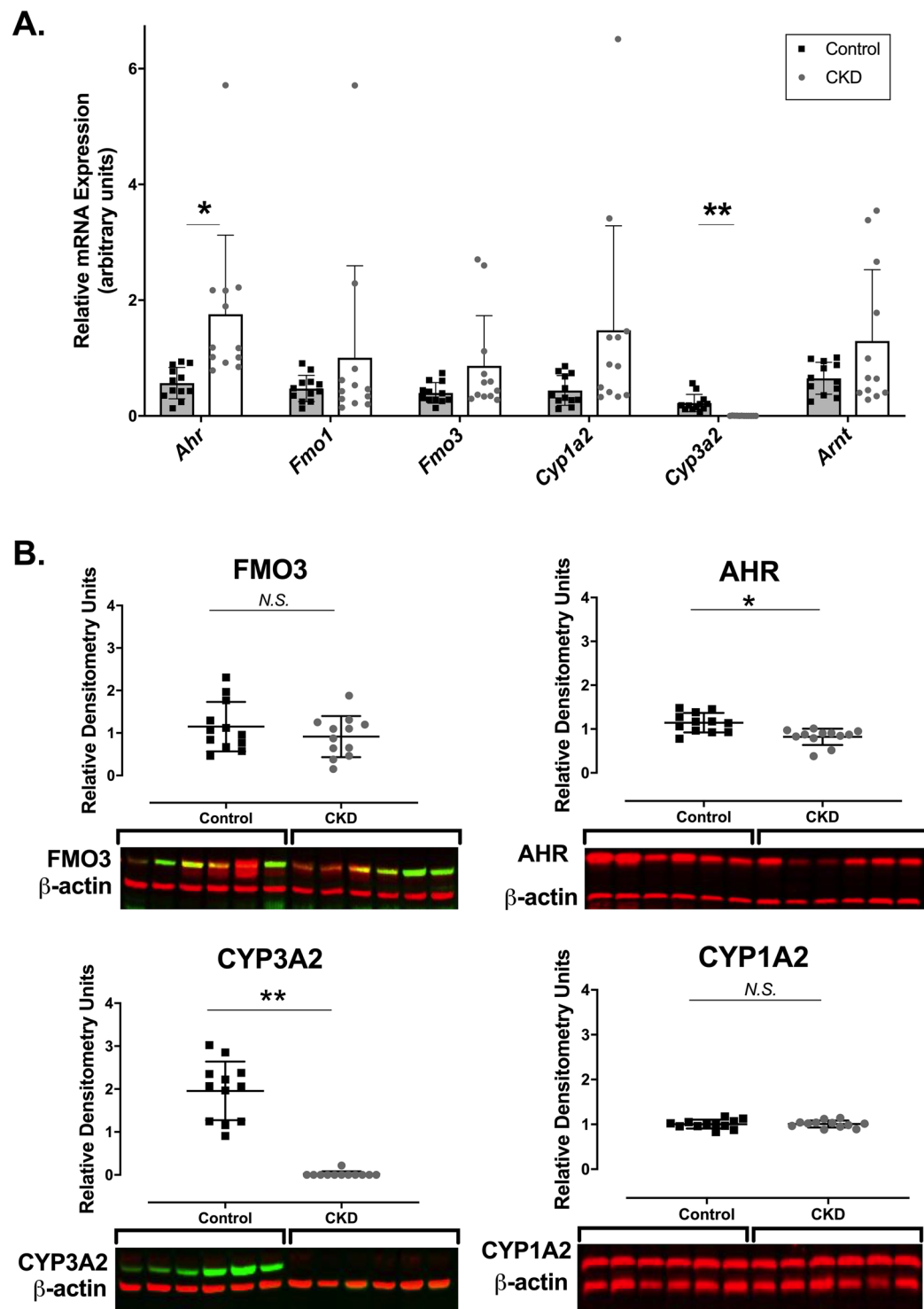
Figure 2. mRNA and Protein Expression. (**A**) mRNA expression of hepatic drug metabolism enzymes and related genes (*Fmo3*, *Fmo1*, *Arnt*, *Ahr*, *Cyp1a2*, *Cyp3a2* and *Actb*) in control and CKD rats. Hepatic mRNA levels were normalized to β-Actin and expressed relative to the controls using absolute quantification. Experiments were conducted in duplicates, and results are presented as mean ± SD of 12 rats in each group. *$P < 0.05$ and **$P < 0.001$ compared with control by Student's *t*-tests. (**B**) Protein expression of drug metabolism enzymes and related proteins (FMO3, AhR, CYP1A2, CYP3A2 and β-Actin) in control and CKD rat livers. The densitometry units of protein expression were normalized to that of β-Actin. The results are presented as mean ± SD of 12 rats in each group. The lower panel represents blots of six control and six CKD rats. *$P < 0.05$ and **$P < 0.001$ compared with control by Student's *t*-tests. The corresponding full-length blots are presented in Supplementary Figures 2–5.

A.
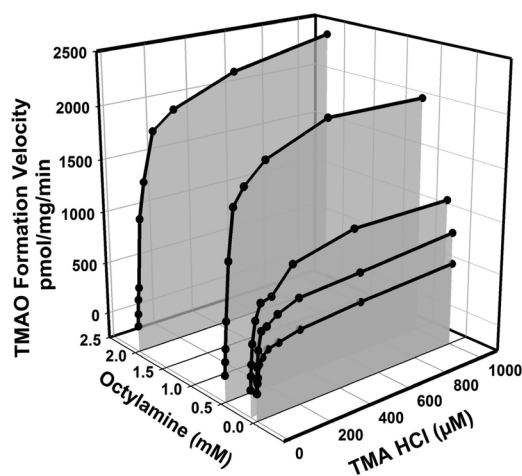
Parameters	Km (SE)	Vmax (SE)	P
Control	13 (2)	488 (15)	—
0.01 mM Octylamine	13 (1)	781 (15)	< 0.0001
0.1 mM Octylamine	23 (3)	1,121 (30)	< 0.0001
0.5 mM Octylamine	28 (2)	2,119 (34)	< 0.0001
2 mM Octylamine	39 (4)	2,437 (60)	< 0.0001

B.
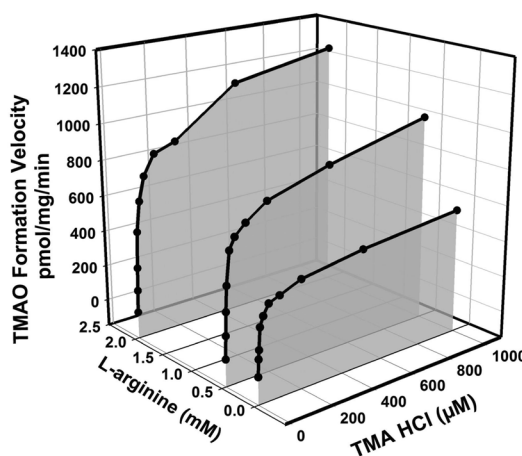
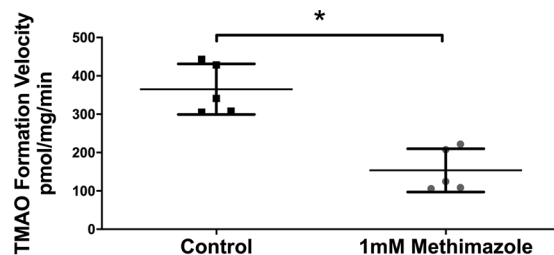| Parameters	Km (SE)	Vmax (SE)	P
Control	13 (2)	488 (15)	—
0.5 mM L-arginine	16 (2)	895 (24)	< 0.0001
2 mM L-arginine	22 (3)	1,156 (34)	< 0.0001

C.

Figure 3. Metabolic Activation and Inhibition of FMO. Michaelis-Menten plot for the formation of TMAO in rat liver microsomes in the presence of increasing concentrations of (**A**) octylamine and (**B**) L-arginine. Liver microsomal protein (0.5 mg/mL) was incubated with various concentrations of trimethylamine (2.5–1000 μM) for 60 min at 37 °C in the presence of either octylamine (0.01–2 mM) or L-arginine (0.5 and 2 mM). Each point represents the mean of at least 3 replicates at each trimethylamine concentration in each group. The parameters were statistically compared with an F-test. Note that P value represents a comparison of Vmax for each octylamine or L-arginine concentration versus control. (**C**) FMO-mediated TMAO formation was also assessed in the presence of the FMO inhibitor methimazole. Liver microsomal protein (0.5 mg/mL) was incubated with 50 μM of trimethylamine for 60 min at 37 °C in the presence of 1 mM of methimazole. Each point represents the mean ± SD of 5 replicates. *$P < 0.001$ for treatment group compared to control by Student's t-test.

In accordance with enzyme kinetic principles, the increased V_{max} resulting from metabolic activation of FMOs would result in a corresponding increase in TMAO formation when substrate (trimethylamine) concentrations exceed the relatively low K_m value (enzyme affinity for substrate) of approximately 28 μM for FMO3 enzymes[33]. In this scenario, the reaction is rate limited and not substrate/supply limited, such that any increase in V_{max} leads
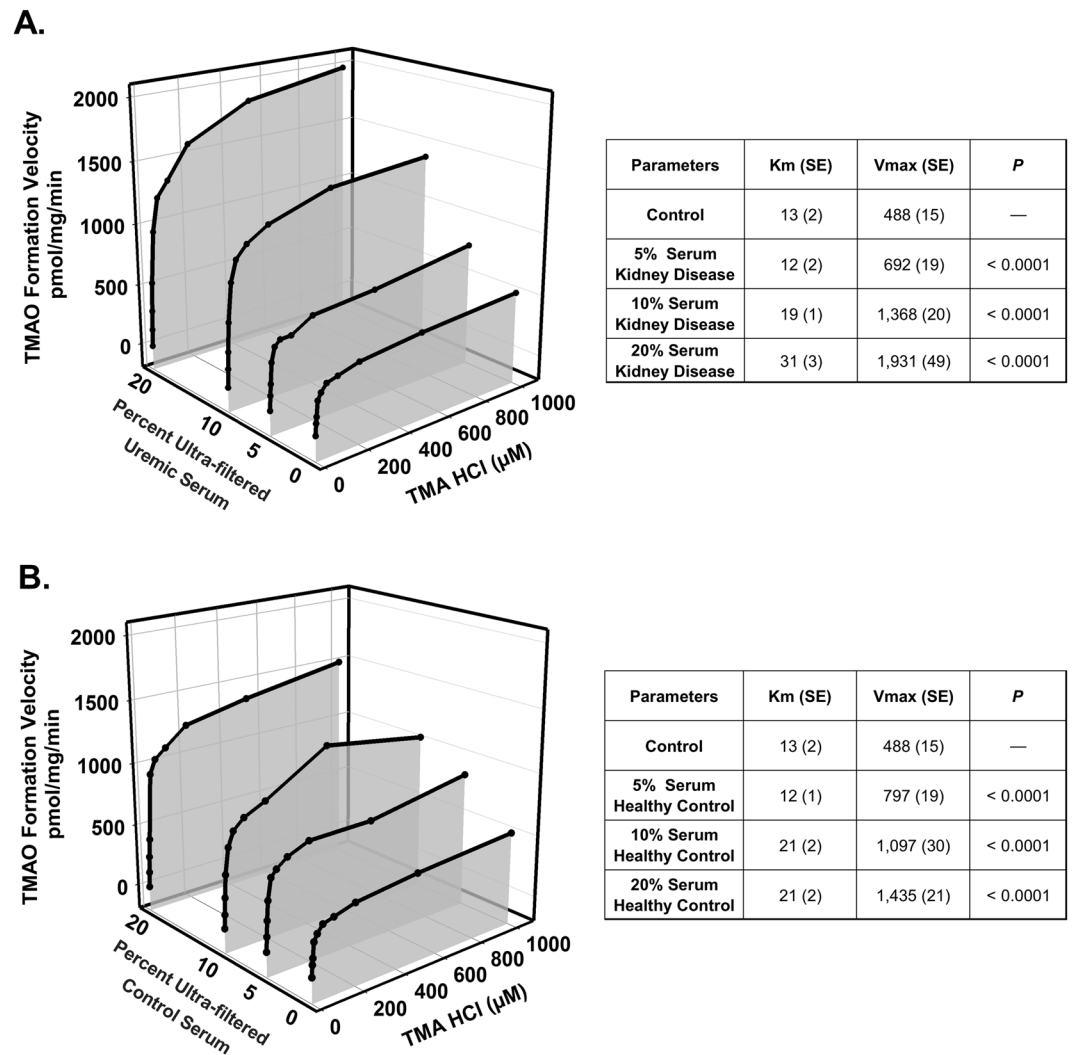
A.

Parameters	Km (SE)	Vmax (SE)	P
Control	13 (2)	488 (15)	—
5% Serum Kidney Disease	12 (2)	692 (19)	< 0.0001
10% Serum Kidney Disease	19 (1)	1,368 (20)	< 0.0001
20% Serum Kidney Disease	31 (3)	1,931 (49)	< 0.0001

B.

Parameters	Km (SE)	Vmax (SE)	P
Control	13 (2)	488 (15)	—
5% Serum Healthy Control	12 (1)	797 (19)	< 0.0001
10% Serum Healthy Control	21 (2)	1,097 (30)	< 0.0001
20% Serum Healthy Control	21 (2)	1,435 (21)	< 0.0001

Figure 4. Metabolic Activation of FMO-mediated TMAO Formation by Human Serum. Michaelis-Menten plots for the formation of TMAO in rat liver microsomes in the presence of increasing percentages of (**A**) human uremic serum and (**B**) healthy control serum. Liver microsomal protein (0.5 mg/mL) was incubated with various concentrations of trimethylamine (2.5–1000 µM) for 60 min at 37 °C in the presence of serum (5–20%). Each point represents the mean of at least 3 replicates at each trimethylamine concentration in each group. The parameters were statistically compared with an F-test. Note that *P* value represents a comparison of Vmax for each percent ultra-filtered serum group versus control.

to a corresponding increase in TMAO formation. Trimethylamine concentrations can exceed this K_m value in humans considering trimethylamine production is approximately 50 mg/day, especially after a precursor-nutrient rich meal[34–36]. Furthermore, FMO3 gene polymorphisms are associated with increased TMAO concentrations, indicating that FMO-mediated TMAO formation is not supply limited[17]. Overall, these data support a novel biologically plausible mechanism involving metabolic activation that increases the V_{max} of FMO-mediated TMAO formation and contributes to well documented increases in systemic concentrations of TMAO in CKD patients.

Although activation of FMOs leads to increased TMAO formation in this experimental model of CKD, this requires validation in humans. We and several other investigators have reported elevated concentrations of trimethylamine and/or TMAO in CKD patients (Supplementary Table S1)[5,7,9,37], but to date the potential mechanisms are unclear. Decreased renal clearance undoubtedly contributes to elevated serum TMAO concentrations[38], although the relative contribution is unclear and likely minimal in the setting of advanced kidney disease. Additionally, the observations that systemic TMAO concentrations increase disproportionately in advanced CKD relative to earlier stages of CKD[9], and that hemodialysis is relatively ineffective at lowering systemic exposure of TMAO (i.e., evidenced by pre-dialysis concentrations)[39], despite high intradialytic clearance[37,40], support the premise that TMAO formation is increased in CKD. It has been postulated that TMAO production is not changed in ESKD patients receiving chronic hemodialysis, and that the extraordinarily increased concentrations in these patients are due partly to the inability of hemodialysis to provide clearances of the magnitude achieved by tubular secretion[40]. While the latter point is valid, TMAO concentrations rise disproportionately even in non-dialyzed Stage 4 CKD patients with residual kidney function and presumably residual secretory clearance. One possible

explanation is that the loss of secretory clearance in ESKD is outweighed by a simultaneous increase in TMAO production leading to the increased systemic exposure observed. Lastly, though decreased nonrenal clearance also may impact the systemic exposure of substrates predominantly cleared by the pathway in question[41], TMAO undergoes little nonrenal clearance[42], so this is unlikely to explain the increases in systemic exposure observed as kidney disease progresses. Overall, high systemic TMAO exposure is likely due to a combination of decreased renal clearance[43], and increased TMAO production in kidney disease.

There are several limitations of the current study. Post-translational modifications like phosphorylation may affect enzyme activity and this was not evaluated. The microbiome plays an integral role in the production of trimethylamine, the FMO substrate that is metabolized into TMAO, and we did not explore how it is changed in CKD or whether any changes are associated with altered TMAO formation. It is also possible that the potential effector compounds may be derived from dietary nutrients. The patients that contributed the uremic and healthy serum were not on a controlled diet, which may have influenced the metabolic activation results. In addition, serum from other donors was not evaluated to replicate these findings. There are hundreds of known uremic retention solutes that accumulate in CKD and future work is necessary to determine the potential effector compounds that may activate FMO-mediated TMAO formation[44]. Future *in vitro* and *in vivo* studies will evaluate FMO enzyme activity in the presence of individual solutes (i.e., TMAO, urea, primary amines, guanidine derivatives, etc.). Lastly, therapeutically targeting FMO3 function by partial inhibition may not induce the undesirable symptoms of trimethylaminuria observed in patients with inactive FMO3 enzymes[35], but this should be carefully evaluated.

In conclusion, we show for the first time that metabolic activation of hepatic FMOs leads to increased formation of the non-traditional CVD risk factor TMAO. These data provide important mechanistic insight into the function of hepatic FMOs, as metabolic activation may contribute to the elevated TMAO concentrations observed as kidney function declines. FMO-mediated metabolism may be a therapeutic target to decrease TMAO exposure and thereby lower rates of CVD in patients with CKD.

Methods

Chemical reagents. Trimethylamine hydrochloride, TMAO, NADPH, magnesium chloride, tris (hydroxymethyl) aminomethane (Trizma® base), Trizma® hydrochloride, n-octylamine, methimazole, L-arginine and formic acid ($\geq 95\%$) were purchased from Sigma-Aldrich (St. Louis, MO). Deuterated internal standard (*d*9-trimethylamine N-oxide) was purchased from Cambridge Isotopes (Cambridge, MA, USA). Optima LC–MS grade water, acetonitrile, and methanol was purchased from Fisher Scientific (Pittsburgh, PA). Taqman® primers used for mRNA quantification were purchased from Applied Biosystems (Foster City, CA). All fluorescent antibodies were purchased from Abcam (Cambridge, MA) (Codes: ab2769, ab8226, ab22717, ab126790, ab195627, ab186693 and ab175774).

Experimental model. Male Sprague-Dawley rats (Charles River, Saint-Charles, PQ, Canada) that weighed 200 to 300 g were fed standard rat chow and water *ad libitum* on a 12-hour light/dark cycle. Control rats were pair-fed matching amounts of standard rat chow consumed by CKD rats. The Canadian Council on Animal Care guidelines were observed for care and use of laboratory animals. The experimental protocol was authorized by the Maisonneuve-Rosemont Hospital Research Centre Animal Care Committee. Experimental CKD was surgically induced by first performing a 2/3rd nephrectomy of the left kidney followed 7 days later by a complete right nephrectomy, as previously described[45]. Control rats underwent to two sham laparotomies. Rats were sacrificed 42 days after the initial surgery and livers were immediately harvested and stored at $-80\,°C$.

Determination of FMO activity. Metabolic activity of hepatic FMOs was assessed with isolated microsomes of control (n = 6) and CKD (n = 6) rat livers. Specifically, trimethylamine was used as a probe substrate of FMO enzymes, and formation rate of TMAO was used as a surrogate measurement of FMO activity. Hepatic microsomes (i.e., the liver fraction containing FMOs) were isolated by differential ultra-centrifugation as previously described[46]. Incubation times and microsomal protein concentrations were optimized to achieve linear formation of TMAO in the experiments. Microsomal incubations using 0.5 mg/mL of microsomal protein in 0.02 M Tris-HCl buffer (pH 7.4) containing 1 mM nicotinamide adenine dinucleotide phosphate (NADPH), as an essential cofactor, and 5 mM magnesium chloride ($MgCl_2$) were conducted for each rat. The microsomal incubations were pre-warmed in the presence of NADPH for 3 minutes at 37 °C. To start the reaction, 3 μL of increasing concentrations of trimethylamine (2.5, 5, 10, 25, 50, 100, 200, 500, 1000 μM) was added, and microsomes were incubated for 60 min at 37 °C. Final reaction volumes were 300 μL. Each trimethylamine incubation experiment (i.e., each concentration) was conducted in duplicate (CKD vs. healthy control). Negative controls omitting NADPH and trimethylamine were assessed for all incubations. Reactions were stopped by adding 300 μL of ice-cold methanol. TMAO was quantified by ultra-performance liquid chromatography tandem mass spectrometry (LC-MS/MS) as we reported previously[47].

mRNA analysis. RNA isolation and real-time quantitative polymerase chain reaction (RT-qPCR) were conducted as recommended by MIQE guidelines[48]. Total RNA was extracted from homogenized liver tissue from n = 12 CKD and n = 12 control rats, using QiaShredder and RNeasy Mini Kit (Qiagen, Valencia, CA). RNA purity (260/280 ratios ranging from 1.8 to 2.0) and concentrations were determined by measuring the optical density at 260 nm and 280 nm using NanoDrop (ThermoFisher Scientific, Waltham, MA). cDNA was then prepared using SuperScript III reverse transcriptase (Invitrogen, San Diego, CA) with 1 μg of total RNA and random hexamers. *Fmo3*, *Fmo1*, *Arnt*, *Ahr*, *Cyp1a2*, *Cyp3a2* and *Actb* (β-Actin) genes were quantified by RT-qPCR with Applied Biosystems 7500 Fast Real-Time PCR System (Foster City, CA) using Taqman® Gene Expression Master Mix (Applied Biosystems, Foster City, CA) and Taqman® specific primers. Template and reverse transcriptase controls

were not included in every reaction. *Ahr* and *Arnt* were selected because the aryl-hydrocarbon receptor (AhR) signaling pathway may be activated in CKD and partially regulate FMO expression[49,50]. Hepatic mRNA concentrations were normalized to *Actb* and expressed relative to the controls using absolute quantification.

Western blot analysis.   The protein expression of hepatic FMO3, CYP1A2, CYP3A2, AHR and β-Actin was determined with fluorescent Western blotting. Homogenized liver tissue from n = 12 CKD and n = 12 control rats (30 μg total protein) were separated by 4–15% Mini Protean TGX (Bio-Rad, Hercules, CA) gel electrophoresis and transferred onto PVDF membranes. Transferred membranes were blocked for 1 hour at room temperature using Odyssey Blocking Buffer. Membranes were incubated at 4 °C overnight with specific primary antibodies diluted in 50:50 blocking buffer and TBS- 0.1% Tween (TBST) (1:1000–2500 mouse monoclonal anti- β-Actin, CYP1A2 and AhR; 1:1000 polyclonal rabbit anti- FMO3 and CYP3A2). Membranes were washed four times for 10 minutes with TBST and then for one hour with 50:50 blocking buffer and TBST. Membranes were then incubated for 1 hour in fluorescent secondary antibodies at room temperature (1:20000 donkey anti-rabbit; or 1:10000 donkey anti-mouse). Finally, membranes were washed with TBST, and antibody binding was measured by a LI-COR fluorescent reader (Lincoln, NE) detection system. CYP1A2 and CYP3A2 were selected as controls because their expression in experimental CKD is unchanged and decreased, respectively[51]. Specificity was assessed by incubating blots that were loaded with control homogenized rat tissue with each primary antibody to check for overlapping fluorescent bands (see Supplementary S-Fig. 1). The linear range of detection was determined for a range of total protein on these blots. Band intensity was quantified by densitometry using ImageJ software and normalized to β-Actin expression.

Assessment of FMO metabolic activation and inhibition.   Metabolic activation was explored as a potential mechanism of increased FMO activity. Metabolic activation was assessed using the experimental conditions described above for the determination of FMO activity. However, male Sprague-Dawley rat liver microsomes (purchased from Sekisui XenoTech, Kansas City, KS) were used in these experiments. The reference point of FMO activity in these microsomes was consistent with the experimental control rats. Also, potential activating compounds (0.01–2 mM octylamine or 0.5 and 2 mM L-arginine), and human serum were added to the microsomal incubations prior to the start of the reaction. The FMO inhibitor methimazole (1 mM) was added to 5 replicates of the 50 μM trimethylamine incubates. TMAO formation rates were assessed to measure changes in FMO metabolic activity.

In experiments with human serum, appropriate volumes were added to achieve the 5, 10 and 20% of total reaction volume. Baseline concentrations of trimethylamine and TMAO in the human serum were quantified before starting the incubation reactions (Supplementary Table S1). Final TMAO formation was calculated by taking the final TMAO concentration minus the baseline TMAO concentration. Concentrations of baseline trimethylamine in serum were below the limit of quantification, and therefore were negligible (Supplementary Table S1). Baseline TMAO did not undergo any quantifiable metabolism or retro-reduction into trimethylamine in the microsomal incubations. Healthy human control serum was purchased from a local blood bank and serum from a hemodialysis patient (pre-dialysis sample; serum creatinine, 14.6 mg/dL; BUN, 77 mg/dL) was obtained with informed consent and approval from the University of Kansas Medical Center Institutional Review Board. All serum was ultra-filtered using 10 Kda Satorius Vivaspin® spin columns.

Data and statistical analysis.   Individual rat serum TMAO concentrations were adjusted based on kidney function by dividing by the corresponding serum creatinine values. The formation rate of TMAO was determined from LC-MS/MS quantified TMAO concentrations in the microsomal incubates. Non-linear regression Michaelis-Menten kinetic models were used to fit FMO-mediated TMAO formation data, and the maximum velocity (V_{max}) and the affinity constant (K_m) were estimated and compared by extra-sum-of-squares F-tests with GraphPad Prism (Version 8.0.2; San Diego, CA). Hepatic mRNA levels were normalized to β-Actin and expressed relative to the controls using absolute quantification. Densitometry units of protein expression were normalized to that of β-Actin. Gene and protein expression were not performed in one control rat liver sample due to limited tissue quantity. Student's *t*-test or Mann-Whitney test for data exhibiting non-normal distribution were used to compare CKD to control rats. *P*-values of < 0.05 were considered significant. All results are presented as mean ± SD, unless otherwise stated.

Data availability
The datasets generated during and/or analyzed during the current study are available from the corresponding author on reasonable request.

References
1. Sarnak, M. J. *et al*. Kidney disease as a risk factor for development of cardiovascular disease: a statement from the American Heart Association Councils on Kidney in Cardiovascular Disease, High Blood Pressure Research, Clinical Cardiology, and Epidemiology and Prevention. *Circulation* **108**, 2154–2169 (2003).
2. Ramezani, A. *et al*. Role of the Gut Microbiome in Uremia: A Potential Therapeutic Target. *Am J Kidney Dis* **67**, 483–498 (2016).
3. Meyer, T. W. & Hostetter, T. H. Approaches to uremia. *J Am Soc Nephrol* **25**, 2151–2158 (2014).
4. Wang, Z. *et al*. Gut flora metabolism of phosphatidylcholine promotes cardiovascular disease. *Nature* **472**, 57–63 (2011).
5. Shafi, T. *et al*. Trimethylamine N-Oxide and Cardiovascular Events in Hemodialysis Patients. *J Am Soc Nephrol* **28**, 321–331 (2017).
6. Tang, W. H. *et al*. Gut microbiota-dependent trimethylamine N-oxide (TMAO) pathway contributes to both development of renal insufficiency and mortality risk in chronic kidney disease. *Circ Res* **116**, 448–455 (2015).

7. Kim, R. B. *et al*. Advanced chronic kidney disease populations have elevated trimethylamine N-oxide levels associated with increased cardiovascular events. *Kidney Int* **89**, 1144–1152 (2016).

8. Tang, W. H. *et al*. Intestinal microbial metabolism of phosphatidylcholine and cardiovascular risk. *N Engl J Med* **368**, 1575–1584 (2013).

9. Stubbs, J. R. *et al*. Serum Trimethylamine-N-Oxide is Elevated in CKD and Correlates with Coronary Atherosclerosis Burden. *J Am Soc Nephrol* **27**, 305–313 (2016).

10. Tang, W. H. *et al*. Intestinal microbiota-dependent phosphatidylcholine metabolites, diastolic dysfunction, and adverse clinical outcomes in chronic systolic heart failure. *J Card Fail* **21**, 91–96 (2015).

11. House, A. A. *et al*. Heart failure in chronic kidney disease: conclusions from a Kidney Disease: Improving Global Outcomes (KDIGO) Controversies Conference. *Kidney Int* **95**, 1304–1317 (2019).

12. Zeisberg, E. M. *et al*. Endothelial-to-mesenchymal transition contributes to cardiac fibrosis. *Nat Med* **13**, 952–961 (2007).

13. Johnson, C., Prokopienko, A. J., West, R. E., III, Nolin, T. D. & Stubbs, J. R. Decreased Kidney Function is Associated with Enhanced Hepatic Flavin Monooxygenase Activity and Increased Circulating Trimethylamine N-oxide Concentrations in Mice. *Drug Metab Dispos* (2018).

14. Ziegler, D. M., Poulsen, L. L. & McKee, E. M. Interaction of primary amines with a mixed-function amine oxidase isolated from pig liver microsomes. *Xenobiotica* **1**, 523–531 (1971).

15. Miao, J. *et al*. Flavin-containing monooxygenase 3 as a potential player in diabetes-associated atherosclerosis. *Nat Commun* **6**, 6498 (2015).

16. Shih, D. M. *et al*. Flavin containing monooxygenase 3 exerts broad effects on glucose and lipid metabolism and atherosclerosis. *J Lipid Res* **56**, 22–37 (2015).

17. Robinson-Cohen, C. *et al*. Association of FMO3 Variants and Trimethylamine N-Oxide Concentration, Disease Progression, and Mortality in CKD Patients. *PLoS One* **11**, e0161074 (2016).

18. Novick, R. M., Mitzey, A. M., Brownfield, M. S. & Elfarra, A. A. Differential localization of flavin-containing monooxygenase (FMO) isoforms 1, 3, and 4 in rat liver and kidney and evidence for expression of FMO4 in mouse, rat, and human liver and kidney microsomes. *J Pharmacol Exp Ther* **329**, 1148–1155 (2009).

19. Randrianarisoa, E. *et al*. Relationship of Serum Trimethylamine N-Oxide (TMAO) Levels with early Atherosclerosis in Humans. *Sci Rep* **6**, 26745 (2016).

20. Ripp, S. L., Itagaki, K., Philpot, R. M. & Elfarra, A. A. Species and sex differences in expression of flavin-containing monooxygenase form 3 in liver and kidney microsomes. *Drug Metab Dispos* **27**, 46–52 (1999).

21. Bennett, B. J. *et al*. Trimethylamine-N-oxide, a metabolite associated with atherosclerosis, exhibits complex genetic and dietary regulation. *Cell Metab* **17**, 49–60 (2013).

22. Kielstein, J. T. *et al*. Marked increase of asymmetric dimethylarginine in patients with incipient primary chronic renal disease. *J Am Soc Nephrol* **13**, 170–176 (2002).

23. Hutzler, J. M., Hauer, M. J. & Tracy, T. S. Dapsone activation of CYP2C9-mediated metabolism: evidence for activation of multiple substrates and a two-site model. *Drug Metab Dispos* **29**, 1029–1034 (2001).

24. Ziegler, D. M., McKee, E. M. & Poulsen, L. L. Microsomal flavoprotein-catalyzed N-oxidation of arylamines. *Drug Metab Dispos* **1**, 314–321 (1973).

25. Ziegler, D. M. & Mitchell, C. H. Microsomal oxidase. IV. Properties of a mixed-function amine oxidase isolated from pig liver microsomes. *Arch Biochem Biophys* **150**, 116–125 (1972).

26. Velenosi, T. J. *et al*. Untargeted plasma and tissue metabolomics in rats with chronic kidney disease given AST-120. *Sci Rep* **6**, 22526 (2016).

27. Prokopienko, A. J. & Nolin, T. D. Microbiota-derived uremic retention solutes: perpetrators of altered nonrenal drug clearance in kidney disease. *Expert Rev Clin Pharmacol* **11**, 71–82 (2018).

28. Pfeifer, N. D., Harris, K. B., Yan, G. Z. & Brouwer, K. L. Determination of intracellular unbound concentrations and subcellular localization of drugs in rat sandwich-cultured hepatocytes compared with liver tissue. *Drug Metab Dispos* **41**, 1949–1956 (2013).

29. Midgley, I. *et al*. Pharmacokinetics and metabolism of the prodrug DB289 (2,5-bis[4-(N-methoxyamidino)phenyl]furan monomaleate) in rat and monkey and its conversion to the antiprotozoal/antifungal drug DB75 (2,5-bis(4-guanylphenyl)furan dihydrochloride). *Drug Metab Dispos* **35**, 955–967 (2007).

30. Nishimura, Y. *et al*. Inhibitory effects of adenine nucleotides and related substances on UDP-glucuronosyltransferase: structure-effect relationships and evidence for an allosteric mechanism. *Biochim Biophys Acta* **1770**, 1557–1566 (2007).

31. Dorner, A. J. & Kaufman, R. J. The levels of endoplasmic reticulum proteins and ATP affect folding and secretion of selective proteins. *Biologicals* **22**, 103–112 (1994).

32. Ishii, Y., An, K., Nishimura, Y. & Yamada, H. ATP serves as an endogenous inhibitor of UDP-glucuronosyltransferase (UGT): a new insight into the latency of UGT. *Drug Metab Dispos* **40**, 2081–2089 (2012).

33. Lang, D. H. *et al*. Isoform specificity of trimethylamine N-oxygenation by human flavin-containing monooxygenase (FMO) and P450 enzymes: selective catalysis by FMO3. *Biochem Pharmacol* **56**, 1005–1012 (1998).

34. Jaworska, K. *et al*. Hypertension in rats is associated with an increased permeability of the colon to TMA, a gut bacteria metabolite. *PLoS One* **12**, e0189310 (2017).

35. Mitchell, S. C. & Smith, R. L. Trimethylaminuria: the fish malodor syndrome. *Drug Metab Dispos* **29**, 517–521 (2001).

36. Fennema, D., Phillips, I. R. & Shephard, E. A. Trimethylamine and Trimethylamine N-Oxide, a Flavin-Containing Monooxygenase 3 (FMO3)-Mediated Host-Microbiome Metabolic Axis Implicated in Health and Disease. *Drug Metab Dispos* **44**, 1839–1850 (2016).

37. Bain, M. A., Faull, R., Fornasini, G., Milne, R. W. & Evans, A. M. Accumulation of trimethylamine and trimethylamine-N-oxide in end-stage renal disease patients undergoing haemodialysis. *Nephrol Dial Transplant* **21**, 1300–1304 (2006).

38. Manor, O. *et al*. A Multi-omic Association Study of Trimethylamine N-Oxide. *Cell Rep* **24**, 935–946 (2018).

39. Sirich, T. L. *et al*. Limited reduction in uremic solute concentrations with increased dialysis frequency and time in the Frequent Hemodialysis Network Daily Trial. *Kidney Int* **91**, 1186–1192 (2017).

40. Hai, X. *et al*. Mechanism of Prominent Trimethylamine Oxide (TMAO) Accumulation in Hemodialysis Patients. *PLoS One* **10**, e0143731 (2015).

41. Nolin, T. D. *et al*. ESRD impairs nonrenal clearance of fexofenadine but not midazolam. *J Am Soc Nephrol* **20**, 2269–2276 (2009).

42. Miyake, T. *et al*. Involvement of Organic Cation Transporters in the Kinetics of Trimethylamine N-oxide. *J Pharm Sci* **106**, 2542–2550 (2017).

43. Teft, W. A. *et al*. Identification and Characterization of Trimethylamine-N-oxide Uptake and Efflux Transporters. *Mol Pharm* **14**, 310–318 (2017).

44. Duranton, F. *et al*. Normal and pathologic concentrations of uremic toxins. *J Am Soc Nephrol* **23**, 1258–1270 (2012).

45. Leblond, F. A., Giroux, L., Villeneuve, J. P. & Pichette, V. Decreased *in vivo* metabolism of drugs in chronic renal failure. *Drug Metab Dispos* **28**, 1317–1320 (2000).

46. Alshogran, O. Y. *et al*. Effect of experimental kidney disease on the functional expression of hepatic reductases. *Drug Metab Dispos* **43**, 100–106 (2015).

47. Ocque, A. J., Stubbs, J. R. & Nolin, T. D. Development and validation of a simple UHPLC-MS/MS method for the simultaneous determination of trimethylamine N-oxide, choline, and betaine in human plasma and urine. *J Pharm Biomed Anal* **109**, 128–135 (2015).

48. Bustin, S. A. *et al.* The MIQE guidelines: minimum information for publication of quantitative real-time PCR experiments. *Clin Chem* **55**, 611–622 (2009).
49. Dou, L. *et al.* Aryl hydrocarbon receptor is activated in patients and mice with chronic kidney disease. *Kidney Int* **93**, 986–999 (2018).
50. Celius, T. *et al.* Aryl hydrocarbon receptor-dependent induction of flavin-containing monooxygenase mRNAs in mouse liver. *Drug Metab Dispos* **36**, 2499–2505 (2008).
51. Leblond, F. *et al.* Downregulation of hepatic cytochrome P450 in chronic renal failure. *J Am Soc Nephrol* **12**, 326–332 (2001).

Acknowledgements

Author contributions

Participated in research design: A.J.P., F.A.L., V.P. and T.D.N.; Conducted experiments: A.J.P., F.A.L., R.E.W. and D.P.S.; Contributed new reagents or analytic tools: J.R.S., F.A.L., V.P. and T.D.N.; Performed data analysis: A.J.P., T.D.N.; Wrote or contributed to the writing of the manuscript: A.J.P., R.E.W., D.P.S., F.A.L., V.P., J.R.S. and T.D.N.; All authors approved the final version of the manuscript.

Competing interests

The authors declare no competing interests.

Additional information

Supplementary information is available for this paper at https://doi.org/10.1038/s41598-019-52032-9.

Correspondence and requests for materials should be addressed to T.D.N.

Reprints and permissions information is available at www.nature.com/reprints.

Publisher's note Springer Nature remains neutral with regard to jurisdictional claims in published maps and institutional affiliations.